Emirates International University EIU

Research Article

Emirates International University Journal Issued. (5) .(2026)
(2026) . (5) مجلة الجامعة الإماراتية الدولية. العدد

Towards Cleaner Cement: A Systematic Review of Limestone Calcined Clay Cement.

Ibrahim Alameri*[1,2]

1. *Department of Civil Engineering, Sana'a University, Sana'a, Yemen*
2. *Department of Civil Engineering, Emirates International University, Sana'a, Yemen.*

Abstract

Decarbonizing the cement industry requires a binder that is both low carbon and globally deployable. LC3 is the only supplementary cementitious material with sufficient geological abundance to meet this challenge. Raw materials are widely available, production demands less energy, and durability performance is well established. This PRISMA 2020 compliant systematic review synthesizes evidence from a large body of peer reviewed studies, covering raw materials, calcination, hydration, mechanical properties, durability, environmental performance, economics, and industrial deployment. LC3-50 reduces GWP by 30–40% per ton, and by approximately 90% per year of marine service on a functional-unit basis. Compressive strength equals OPC at 28 days. Chloride diffusivity drops by 10 to 100 times, while basic creep compliance is 28–30% lower than OPC at paste level. Despite these advantages, critical gaps remain in freeze-thaw, creep, fire performance, and non-tropical carbonation. A three-horizon roadmap is proposed to address these gaps. At 20–30% global deployment, LC3 could cut annual CO_2 emissions by 800–900 million tones. The evidence positions LC3 as the most scalable near-term low carbon cement technology.

Keywords

LC3; SCMs; low-carbon cement; life cycle assessment; durability; circular economy.

Received	01/01/2026
Accepted	01/01/2026
Published	31/07/2026
Publisher	Emirates International University

ISSN	3104-6142
ISSN (Online)	3104-6150
DOI	10.64059/eiu.v3i1.100
Wikidata	Q137945151
ROR	03j6pc929

Citation:

Alameri, I. (2026). Towards Cleaner Cement: A Systematic Review of Limestone Calcined Clay Cement. Emirates International University Journal, 3(1), 21. https://doi.org/10.64059/eiu.v3i1.100

Corresponding author

Dr.Ibrahim Alameri, Emirates International University, Yemen, Sana'a.
i.ameri@eiu.edu.ye

Code:

9773104615005

نحو إسمنت أكثر نظافة: مراجعة منهجية لإسمنت الحجر الجيري والطين المكلسن

إبراهيم العامري * [1،2]

1. قسم الهندسة المدنية، جامعة صنعاء، صنعاء، اليمن
2. قسم الهندسة المدنية، الجامعة الإماراتية الدولية، صنعاء، اليمن

الملخص

يتطلب التوجه نحو إزالة الكربون من صناعة الأسمنت مادة رابطة تمتاز بانخفاض البصمة الكربونية وقابلية التطبيق على نطاق عالمي. ويُعد أسمنت الطين المكلسن والحجر الجيري (LC3) المادة الإسمنتية التكميلية الوحيدة التي تتمتع بوفرة جيولوجية كافية لمواجهة هذا التحدي؛ حيث تتوافر موادها الخام على نطاق واسع، وتتطلب عملية إنتاجها طاقة أقل، فضلاً عن أداء ديمومتها المُثبت والموثوق.

تستخلص هذه المراجعة المنهجية، المتوافقة مع معايير(PRISMA 2020) ، الأدلة من مجموعة كبيرة من الدراسات الخاضعة لمراجعة الأقران؛ لتشمل المواد الخام، والتكليس، والإماهة، والخصائص الميكانيكية، والديمومة، والأداء البيئي، والجوانب الاقتصادية، والنشر الصناعي. يقلل نظام (LC3-50)من احتمالية الاحترار العالمي (GWP) بنسبة تتراوح بين 30-40% لكل طن، وبنسبة تقارب 90% لكل عام من الخدمة البحرية على أساس الوحدة الوظيفية. كما تعادل مقاومة الانضغاط لديه تلك الخاصة بالأسمنت البورتلاندي العادي (OPC) عند عمر 28 يوماً. وتنخفض انتشارية الكلوريدات بمقدار 10 إلى 100 مرة، في حين أن امتثال الزحف الأساسي يقل بنسبة 28-30% مقارنة بالأسمنت البورتلاندي العادي على مستوى عجينة الأسمنت.

وعلى الرغم من هذه المزايا، لا تزال هناك فجوات حرجة فيما يتعلق بمقاومة التجمد والذوبان، والزحف، وأداء مقاومة الحريق، والكربنة في البيئات غير الاستوائية. وبناءً على ذلك، تُقترح خارطة طريق تمتد عبر ثلاثة آفاق زمنية لمعالجة هذه الفجوات. وعند بلوغ نسبة اعتماد عالمية تتراوح بين 20-30%، يمكن لأسمنت (LC3) خفض انبعاثات ثاني أكسيد الكربون السنوية بمقدار 800-900 مليون طن. وتؤكد هذه الأدلة مكانة (LC3)باعتبارها تكنولوجيا الأسمنت منخفض الكربون الأكثر قابلية للتوسع في المدى القريب.

الكلمات المفتاحية

إسمنت الحجر الجيري والطين المكلسن؛ LC3؛ المواد الإسمنتية التكميلية؛ الإسمنت منخفض الكربون؛ تقييم دورة الحياة؛ المتانة؛ الاقتصاد الدائري.

Abbreviations

Abbreviation	Definition	Abbreviation	Definition
AFm	aluminate ferrite monosulfate phase	AFt	aluminate ferrite trisulfate (ettringite)
AMBT	accelerated mortar bar test	C-(A)-S-H	aluminium-substituted calcium silicate hydrate
Ccrit	critical chloride threshold	CPT	concrete prism test
D_{nssm}	non-steady-state chloride migration coefficient	DSC	differential scanning calorimetry
FA	fly ash	GGBS	ground granulated blast-furnace slag
GWP	global warming potential	Hc	hemicarbonate
kc(θ)	normalised compressive strength reduction factor	kE(θ)	normalised elastic modulus reduction factor
LC3	limestone calcined clay cement	LC3-50	LC3 with 50% clinker substitution
LCA	life cycle assessment	Mc	monocarbonate

MIP	mercury intrusion porosimetry	MK	metakaolin
NMR	nuclear magnetic resonance spectroscopy	OPC	ordinary Portland cement
PAI	pozzolanic activity index	PCE	polycarboxylate-ether superplasticiser
PRISMA	Preferred Reporting Items for Systematic Reviews	R3 test	rapid, relevant, reliable reactivity test
RCPT	rapid chloride permeability test	RILEM	Réunion Internationale des Laboratoires
ROCE	return on capital employed	SCM	supplementary cementitious material
SP	superplasticiser	TGA	thermogravimetric analysis
TSA	thaumasite form of sulfate attack	w/b	water-to-binder ratio
XRD	X-ray diffraction	XRF	X-ray fluorescence spectrometry
^{27}Al NMR	aluminium-27 solid-state NMR spectroscopy		

1. Introduction

The production of ordinary Portland cement (OPC) is widely recognised as one of the most carbon-intensive industrial processes on Earth(Alameri & Oltulu, 2020b). Projections indicate that global cement output will reach approximately 4.83 billion tonnes per year by 2030, driven principally by accelerating urbanisation across the Global (Manosa et al., 2024; Schneider et al., 2011) , Clinker production requires sustained kiln temperatures of approximately 1450°C, and the process is doubly carbon-intensive. The decomposition of limestone accounts for about 60% of total process emissions, while the combustion of fossil fuels to maintain kiln temperatures contribute the remaining 40% (Scrivener et al., 2018) . Consequently, the cement sector is responsible for an estimated 7–8% of all anthropogenic CO_2 emissions worldwide, rendering it one of the largest single industrial sources (Habert et al., 2020) . A 50% reduction in CO_2 emissions across the cement and concrete value chain can be achieved without huge capital investments, provided that supplementary cementitious materials (SCMs) are used on a large scale(Alameri & Oltulu, 2020a, 2020b; Alameri & Oltulu, 2023).

Partial substitution of clinker with SCMs is widely regarded as the most immediate and cost-effective decarbonisation route available. SCMs react with calcium hydroxide ($Ca(OH)_2$) released during clinker hydration through pozzolanic reactions, forming additional cementitious phases while displacing the carbon-intensive clinker (Lothenbach et al., 2011) . However, the three dominant industrial SCMs face structural supply constraints that are likely to intensify in the coming decade. Fly ash supply is tied to coal-fired power generation, which is declining globally as electricity systems decarbonise. Ground granulated blast-furnace slag (GGBS) production depends on integrated blast-furnace steelmaking routes that are being displaced by electric arc furnace technology with lower slag yields. Silica fume is produced as a by-product of silicon metal and ferrosilicon alloy manufacturing, in quantities orders of magnitude below cement demand (Juenger et al., 2019; Scrivener et al., 2019). Given these constraints, calcined clays emerge as the only SCM category possessing the geological abundance, geographical ubiquity, and pozzolanic quality necessary to fill the supply gap at the scale required to meet cement decarbonisation targets.

The transformative advance that positioned calcined clay at the forefront of next-generation SCMs is the limestone calcined clay cement (LC3) concept, first demonstrated systematically by (Antoni et al., 2012) . They showed that a ternary blend of 30% calcined kaolinitic clay (metakaolin) and 15% limestone with 55% Portland clinker achieved better mechanical properties at 7 and 28 days than pure OPC. This improvement arises from a

synergistic reaction unique to the ternary system. The LC3-50 formulation was subsequently formalised and validated at industrial scale through collaborative research between EPFL, IIT Delhi, IIT Madras, and Universidad Central de Las Villas, Cuba. Independent life-cycle assessments consistently quantify the CO_2 reduction potential of LC3-50 at 30–40% per tonne of binder relative to OPC (Cancio Díaz et al., 2017; Sánchez Berriel et al., 2016) . This review pursues seven interconnected objectives. Evidence on LC3 raw materials, calcination routes, energy demand, and circular economy use of waste-based calcined clay SCMs is synthesised. Hydration mechanisms, microstructural development, and pore structure evolution are compared with OPC and conventional blended systems. Mechanical performance is evaluated, including compressive strength development, elastic modulus relevant to design, and long-term creep and shrinkage behaviour. Durability performance is consolidated across major degradation mechanisms, with emphasis on gaps not fully addressed in earlier studies. Environmental performance is assessed using global warming potential and full life-cycle assessment indicators, including water footprint and related impact categories. Global industrial deployment and economic feasibility are reviewed across different market contexts. A research roadmap is proposed to address six critical knowledge gaps limiting full-scale responsible deployment.

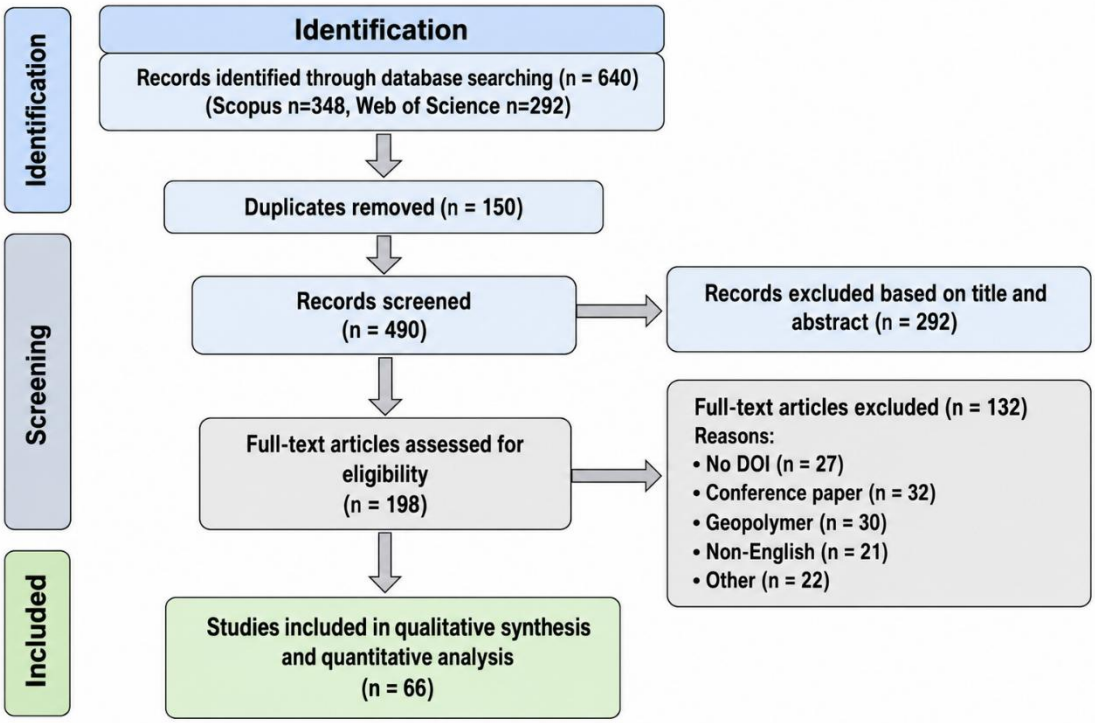

Figure 1 : PRISMA 2020 flow diagram

To address these objectives, a systematic literature search was conducted following the PRISMA 2020 guidelines. The search was performed simultaneously in Scopus and Web of Science, using the search string: ('calcined clay' OR 'metakaolin' OR 'LC3' OR 'limestone calcined clay cement') AND ('supplementary cementitious' OR 'SCM' OR 'pozzolan') AND ('mechanical' OR 'durability' OR 'hydration' OR 'sustainability' OR 'chloride' OR 'carbonation' OR 'life cycle' OR 'freeze-thaw'). The final evidence base consists of 66 peer-reviewed studies, selected after full-text screening and eligibility assessment. **Figure 1** presents the PRISMA 2020 (Page et al., 2021) flow diagram summarising this selection process.

2. Raw Material Characterization and Clay Mineralogy Research Methodology

2.1 Clay Mineral Structure and Pozzolanic Activation Mechanisms

The performance of any calcined clay SCM is governed fundamentally by the mineralogy of the parent clay before calcination. Clay minerals are phyllosilicates built from alternating tetrahedral Si-O sheets and octahedral $Al(OH)_2$ sheets. Kaolinite ($Al_2Si_2O_5(OH)_4$) is a 1:1 dioctahedral phyllosilicate whose controlled thermal treatment at 600–850°C drives dehydroxylation to produce metakaolin ($Al_2Si_2O_7$), a disordered aluminosilicate in which aluminium adopts five-fold (Al(V)) coordination alongside four-fold (Al(IV)) environments (Fernandez et al., 2011; Overmann et al., 2024). This Al(V) coordination state is the definitive indicator of pozzolanic reactivity and is uniquely detectable by ^{27}Al solid-state NMR spectroscopy, which provides the most reliable quantification of reactive alumina available for downstream carboaluminate and C-(A)-S-H formation (Overmann et al., 2024; Snellings et al., 2022).

(Fernandez et al., 2011) conducted the foundational comparative calcination study of kaolinite, illite, and montmorillonite, demonstrating that kaolinite undergoes a fundamentally more complete crystallinity loss under equivalent thermal conditions. Kaolinite dehydroxylation is endothermic and effectively irreversible below approximately 900°C, producing a pseudo-amorphous material with high reactive surface area and Al(V) content. Illite dehydroxylation is partial and produces less reactive metastable phases, while montmorillonite retains residual ordering that limits Al(V) formation. These structural differences translate directly to pozzolanic activity rankings: kaolinite consistently exceeds the ASTM C618 75% pozzolanic activity index (PAI) threshold, whereas illite rarely achieves this benchmark independently (Hollanders et al., 2016). Halloysite ($Al_2Si_2O_5(OH)_4 \cdot 2H_2O$), a tubular 1:1 aluminosilicate related to kaolinite, achieves high reactivity at 600–750°C because its structural water facilitates complete dehydroxylation at lower temperatures (Hollanders et al., 2016). Iron oxide (Fe_2O_3) impurities present in natural clay deposits accelerate sintering onset, narrow the effective calcination window, and contribute to the reddish-brown colouration of LC3 concrete that creates aesthetic acceptance barriers in architectural applications; deposits with Fe_2O_3 above approximately 8% require specific calcination temperature adjustment (Alujas Diaz et al., 2022).

2.2 Low-Grade Clays, Impurity Phases, and Deposit Screening

Commercially pure kaolinite is a limited and often costly mineral commodity. Therefore, the large-scale viability of LC3 depends critically on the use of low- and medium-grade kaolinitic clays. (Tironi et al., 2012) systematically characterised five Argentine kaolinitic clays spanning kaolinite contents from 17% to 74%, demonstrating a strong positive correlation between kaolinite content and pozzolanic activity (**Figure 2**).(Alujas et al., 2015) extended this analysis to a Cuban clay with approximately 40% kaolinite, confirming peak pozzolanic reactivity at 800°C and establishing that low-grade deposits are viable LC3 precursors. (Zheng et al., 2022) pushed this finding further, demonstrating significant pozzolanic activity at 700–800°C for a Chinese low-grade clay containing only 14.6% kaolinite, confirming that even very low kaolinite contents can yield useful pozzolanic activity when calcination conditions are optimised. The RILEM TC 282-CCL review established that kaolinite contents above approximately 40% deliver reliably high and consistent PAI after thermal activation (Alujas Diaz et al., 2022).

(Hollanders et al., 2016) provided the most systematic comparative dataset on pure calcined clay reactivity, testing eight reference clay samples across 500–900°C and establishing that crystallographic ordering is the primary determinant of both reaction rate and optimal calcination temperature. A critical methodological finding was that the Chapelle test systematically overestimates the pozzolanic reactivity of smectitic and illitic clays relative to the Frattini test, with practical implications for deposit pre-screening when XRD Rietveld refinement is unavailable. The R3 test developed by (Avet et al., 2016) provides a validated rapid industrial screening method that correlates strongly with 28-day and 90-day compressive strength across kaolinite contents from 0% to 95%, making it the most practically useful tool for production quality control. A hierarchical deposit screening protocol combining XRF elemental analysis, XRD Rietveld refinement for kaolinite fraction quantification, Frattini or R3 test as primary pozzolanic reactivity screen, and ^{27}Al NMR for research-grade validation represents the recommended framework (Alujas Diaz et al., 2022; Avet et al., 2016).

Waste-derived and non-conventional clay sources present a significant frontier opportunity for circular economy implementation. (Dixit et al., 2021) demonstrated the viability of waste marine excavation clays from

Singapore (kaolinite 29–61%), achieving 20–60% improvement in chloride penetration resistance at 30% replacement. (Amar et al., 2024) demonstrated that excavated Ypresian clay soils from the Grand Paris Express (GPE) construction project meet pozzolanic activity criteria and achieve compressive strength parity with commercial LC3 formulations; under system expansion life cycle assessment, these waste-derived clays approach zero or negative effective GWP owing to avoided landfill and virgin material displacement credits. The (Sui et al., 2024) empirical model linking calcination temperature and duration to metakaolin transformation ratio and energy consumption provides a practical engineering tool for production optimisation of low-grade deposits. Table 1 summarises the principal clay mineral types as LC3 precursors.

Table 1: Principal clay mineral types as LC3 precursors

Clay Mineral	Opt. T (°C)	PAI (%)	Reactive Phase	Key Limitation
Kaolinite (high-grade)	650–850	90–97	Metakaolin ($Al_2Si_2O_7$)	Limited high-grade deposits; Fe_2O_3 >8% narrows window
Kaolinite (low-grade)	700–900	70–88	Amorphous aluminosilicate	Requires deposit-specific calcination optimisation; Chapelle overestimates PAI
Halloysite	600–750	85–92	Metahalloysite	Less widespread deposits; hydrated form reactive at lower temperature
Montmorillonite	680–820	60–70	Amorphous Si/Al phases	Lower Al(V) yield; mechanochemical activation improves performance substantially
Illite	800–950	50–60	Amorphous aluminosilicate	Rarely meets ASTM C618 independently; benefits from mechanochemical milling
Waste / mixed-layer	750–950	60–80	Mixed amorphous phases	Highly variable; site-specific optimisation essential; LCA credits available

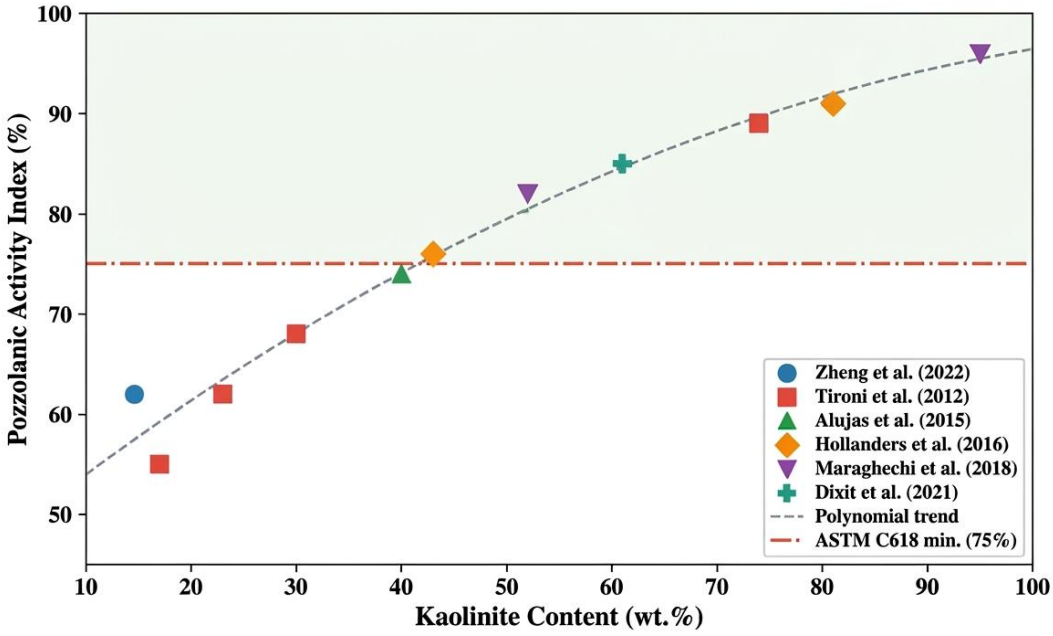

Figure 2 : Pozzolanic activity index (PAI) versus kaolinite content for multiple calcined clay studies

The study relied on the experimental method to measure server performance before and after implementing structural updates. A testing environment simulating live servers was prepared, where a comprehensive system upgrade to version 3.5.0.4 was executed. The methodological procedures included the following:

- Secure access to the servers via the SSH protocol to execute direct upgrade commands.
- Using the package manager (Composer) to automatically process and resolve software dependencies conflicts.

- Clearing template caches and reconfiguring the (php.ini) file directives to comply with the requirements of the new version(Al-Salfi, 2024).
- Monitoring server performance using advanced scanning protocols to ensure the stability of security certificates (SSL/TLS),(Al-Jabri, 2025).

3. Calcination Methods

The conversion of raw clay into a reactive pozzolanic SCM requires controlled thermal activation that destroys the ordered phyllosilicate lattice while stopping short of sintering and recrystallisation reactions. Three principal activation routes are established at industrial and semi-industrial scale: soak (conventional stationary or rotary kiln) calcination, flash (suspension) calcination, and mechanochemical activation. Waste-derived materials represent a fourth, circular economy pathway of growing practical importance. A comprehensive understanding of energy intensity across these routes is essential for accurate life cycle assessment and deployment economics. Table 2 compares the key characteristics of each route.

Table 2 : Comparison of calcination routes for LC3 production

Route	PAI (%)	Thermal Energy (GJ/t)	Electrical Energy (kWh/t)	Capital Cost	Throughput	Best Application
Static kiln (soak)	≥85	2.3–2.6	20–30	Low (retrofit)	Low–Medium	Pilot; existing infrastructure
Rotary kiln (soak)	≥85	2.0–2.5	25–40	Medium (retrofit)	Medium–High	Low-grade clay; existing cement plants
Flash suspension	≥85	1.8–2.2	30–55	High (new)	Very High	Large-scale; fine material streams
Mechanochemical	60–75	0 (ambient)	40–80	Medium	Low	2:1 clay minerals; waste streams
Waste-derived (flash)	60–80	1.8–2.2	30–55	High (new)	High	Circular economy; near-zero GWP

3.1 Soak Calcination

Soak calcination involves slow heating of clay in stationary or rotary kilns over residence times of minutes to hours at 650-900°C. (Almenares et al., 2017) documented the first fully recorded industrial soak calcination trial at the Siguaney Cement Plant in Cuba. Confirming that reactive calcined clay can be produced through modest modifications to existing clinker plant equipment without capital-intensive new kiln construction. The thermal energy demand of soak calcination for kaolinitic clays is approximately 2.0-2.5 GJ per tonne of calcined clay, in comparison with approximately 3.2 GJ per tonne for Portland clinker production, a 25-40% thermal energy reduction Post-calcination grinding, typically requiring 25-40 kWh per tonne to achieve target Blaine fineness, must be included in complete energy balance calculations (Hanein et al., 2021) .The primary limitation of soak calcination is particle agglomeration during slow heating, which reduces effective specific surface area relative to disaggregated product and somewhat reduces early-age reactivity. However, this effect is negligible by 28 days at equivalent dehydroxylation degree (Martirena Hernández et al., 2024).(Krishnan et al., 2019) confirmed industrial scale-up at three Indian locations, establishing soak calcination in retrofitted rotary kilns as the most economically accessible route for emerging-economy deployment.

Maintaining the calcination window is critical because both undercalcination and overcalcination reduce pozzolanic activity. For soak calcination, (Zunino & Scrivener, 2024) conducted systematic investigations across 650-1050°C, establishing that reactivity decline above approximately 950°C is attributable primarily to aluminium-silicon spinel formation, not only to mullite crystallization as previously assumed. The spinel formation onset temperature is clay-specific, occurring between 920°C and 1000°C depending on iron and

magnesium content. Differential scanning calorimetry (DSC) is the most robust industrial quality control tool for detecting overcalculation in soak kilns, and the R3 test (Avet et al., 2016) provides a validated direct reactivity screen that captures the combined effects of dihydroxylation degree, specific surface area, and overcalculation.

3.2 Flash Calcination

Flash calcination involves rapid heating of finely pre-ground clay particles suspended in a hot gas stream for residence times of 1-10 seconds at 800-1000°C, followed by rapid quenching. The thermal energy demand of flash calcination is approximately 1.8-2.2 GJ per tonne owing to more efficient heat transfer to suspended particles. However, the electrical energy demand of pre-grinding and gas circulation typically adds 30-55 kWh per tonne (Hanein et al., 2021). A comparison by (Koutsouradi et al., 2025) across four natural clay types found negligible performance differences between soak and flash routes when samples were compared at equivalent dehydroxylation degree and particle size. Their conclusion was that kaolinite content dominates outcome variability far more than calcination route. (Martirena Hernández et al., 2024) confirmed that there was no major differences in heat of hydration, portlandite consumption, or hydrate phase assemblage between fully dehydroxylated flash and soak-calcined material from the same clay source. The primary practical advantage of flash calcination is its higher throughput capacity and suitability for fine material streams.

For flash calcination, overcalculation risk is also present, but the short residence time reduces the window for spinel formation. Nevertheless, the same upper temperature limit (approximately 950°C) applies, and rapid quenching after calcination is essential to prevent recrystallisation. The R3 test is particularly well suited for flash calcination quality control because it integrates the effects of dihydroxylation degree, particle size distribution, and any overcalculation that may have occurred during the brief high-temperature exposure. Together, DSC (for soak) and R3 testing (for both routes) constitute the minimum recommended analytical package for industrial calcination quality assurance.

3.3 Mechanochemical Activation

Mechanochemical (grinding-induced) activation is particularly effective for 2:1 clay mineral, such as muscovite and montmorillonite through surface aluminium enrichment, lattice strain accumulation, and reduction of Si-O and Al-O binding energies.(Baki et al., 2022) demonstrated that mechanochemical milling enables previously unusable 2:1 clay types to achieve adequate pozzolanic activity, substantially expanding the geological range of deployable raw materials. The electrical energy demand of intensive milling is significant (typically 40-80 kWh per tonne depending on target fineness and mineralogy) and must be accounted for in LCA calculations. Unlike thermal calcination, mechanochemical activation has no risk of overcalculation, but it requires careful control of milling duration and energy input to avoid amorphous phase re-agglomeration.

3.4 Waste-Derived Materials and Circular Economy Pathways

Waste-derived calcined clay SCMs represent a major circular economy opportunity. Flash-calcined dredging sediments (Snellings et al., 2023) , waste marine excavation clays (Dixit et al., 2021) , and Grand Paris Express project soils (Amar et al., 2024) have all demonstrated pozzolanic activity meeting Chapelle and Frattini criteria. Under system expansion LCA approaches, the allocation of avoided burden credits for waste derived clays can reduce effective GWP for these SCMs to near zero or below. This represents the most environmentally favourable production pathway available.

4. Hydration Mechanisms and Microstructural Evolution

The exceptional performance of LC3 systems originates in a hydration chemistry that differs fundamentally from both plain Portland cement and conventional binary SCM blends. The defining feature is a synergistic reaction between reactive alumina supplied by metakaolin and calcium carbonate supplied by limestone, which

together produce a phase assemblage and microstructure that more than compensate for the substantially reduced clinker content (Antoni et al., 2012) . Understanding this mechanism is essential for interpreting all downstream performance characteristics.

4.1 Synergistic Carboaluminate Reaction

The carboalumination reaction was first identified by (Antoni et al., 2012) as the dominant mechanism in LC3 hydration. A combination of XRD, TGA, MIP, and isothermal calorimetry was used to demonstrate that carbonate ions released by limestone dissolution compete with sulphate for reaction with reactive alumina from metakaolin. As a result of this competition, the formation of hemicarbonate (Hc) and monocarbonate (Mc) phases is driven. These two phases stabilise ettringite and increase the total volume of solid hydrates.(De Weerdt et al., 2011) confirmed through TGA, XRD, and pore solution analysis that limestone amplifies carboaluminate formation in ternary systems and increases total hydrate volume compared with binary or plain systems. (Zunino & Scrivener, 2024) established through thermodynamic analysis and systematic experimental characterisation that the carboaluminate reaction is thermodynamically favoured in LC3 systems and that its extent directly governs the degree of porosity refinement and mechanical strength gain. (Overmann et al., 2024) demonstrated that higher-reactivity clays produce greater proportions of Mc and Hc at earlier ages, accelerating pore refinement. (Vizcaíno Andrés et al., 2015) showed that finer limestone provides greater reactive surface area for carbonate dissolution, accelerating early Hc and Mc formation. The water-to-binder (w/b) ratio modulates this reaction: at lower w/b ratios the reduced initial pore solution volume concentrates ionic species and accelerates carboaluminate formation (Hay & Celik, 2023) . Aluminium substitution into C-S-H bridging sites produces C-(A)-S-H, a denser and less permeable gel than OPC C-S-H, with direct implications for chloride transport (Lothenbach et al., 2011).

4.2 Hydration Kinetics and Rate-Limiting Mechanisms

The rate at which LC3 hydrates is controlled by a combination of clinker hydration and pozzolanic reaction, with temperature and clay reactivity being the dominant factors.(Avet & Scrivener, 2018) established a critical quantitative finding: when the calcined kaolinite fraction in the calcined clay exceeds approximately 65%, further clinker reaction is inhibited from three days onwards because the pore structure becomes so refined that the critical pore entry radius reaches approximately 3-5 nm, limiting water transport to unhydrated clinker surfaces. This has profound practical significance: calcined clays with 40-50% kaolinite are sufficient to achieve the full LC3 performance benefit at 28 days and beyond, making high-purity kaolinite unnecessary for practical deployment (Scrivener et al., 2019) . At late ages, (Briki et al., 2021) identified that elimination of water-filled capillary pores above 13 nm radius constrains hydrate growth, confirming that late-age LC3 strength gain is capillary-transport-limited rather than reactant-limited. Temperature exerts a dominant influence on LC3 hydration kinetics. At 10°C, metakaolin pozzolanic dissolution is substantially suppressed, with an apparent activation energy of approximately 45-50 kJ/mol, compared with 30-35 kJ/mol for OPC clinker hydration. Consequently, the pozzolanic contribution to strength at 28 days may be insufficient to achieve OPC equivalence without chemical acceleration or extended curing (Zunino & Scrivener, 2024) . This cold-weather vulnerability represents one of the six priority knowledge gaps identified in this review. **Figure 3** presents a schematic isothermal calorimetry response comparing LC3-50 and OPC.

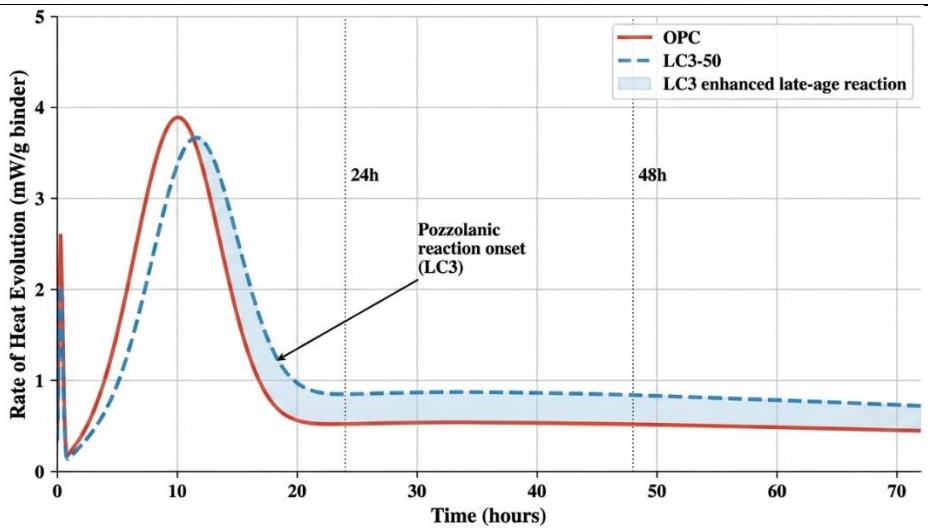

Figure 3 : Schematic isothermal calorimetry response of LC3-50 versus OPC

4.3 Pore Structure Refinement and Transport Properties

The microstructural consequence of carboaluminate and C-(A)-S-H forming reactions is a dramatic progressive refinement of the capillary pore network. (Dhandapani et al., 2018) demonstrated through mercury intrusion porosimetry (MIP) that the critical pore entry diameter decreases from approximately 80–120 nm in OPC at 28 days to approximately 10–30 nm in LC3-50 at the same age, continuing to decrease towards 10 nm by 90 days (**Figure 4**). In addition, bulk electrical resistivity of LC3 concrete at 28 days reaches 55–180 kΩ·cm compared with 4–7 kΩ·cm for OPC, a 10–25-fold improvement that dramatically restricts ionic transport. The extreme pore refinement achieved in LC3 has important positive implications for chloride and sulfate resistance, but raises mechanistic concerns for freeze-thaw performance that are addressed in Section 6.7.

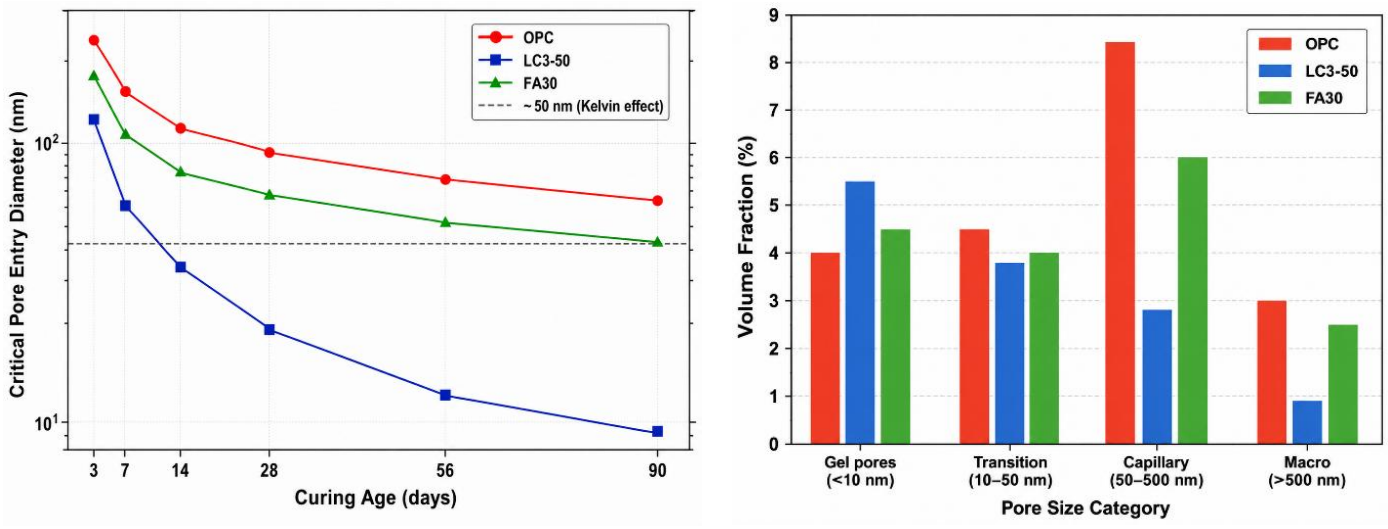

(a) (b)

Figure 4 : (a) Critical pore diameter evolution with curing age (b) porosity decomposition at 28 days for OPC, LC3-50, and FA30 at w/b = 0.45

5. Mechanical Performance

The mechanical performance of LC3 concrete is characterised by an early-age strength deficit arising from lower clinker content and delayed pozzolanic reaction onset, followed by progressive strength gain that reaches and exceeds OPC equivalence at 28 days, and continues to exceed OPC at later ages as pore refinement and pozzolanic reaction advance (Nguyen et al., 2020) . **Table 3** presents key mechanical and durability metrics from primary studies. **Table 4** presents pooled performance data across the validated reference corpus.

5.1 Compressive Strength Development

At one day, LC3-50 achieves approximately 60–65% of OPC one-day strength at equivalent w/b ratio, primarily because the pozzolanic reaction of metakaolin requires an alkaline pore solution established by clinker hydration, creating an inherent early delay before pozzolanic contributions begin. Dhandapani et al. (2018) reported 9 MPa versus 14 MPa at one day for M30 grade (w/b = 0.50), and 14 MPa versus 22 MPa for M50 grade (w/b = 0.35). By 28 days, LC3-50 reaches comparable strength to OPC across M30–M50 grades; beyond 28 days, continued metakaolin reaction and pore refinement drive LC3 strength consistently above OPC, with one-year values 5–18% higher than OPC at equivalent grade across multiple independent studies (Joseph et al., 2023; Sharma et al., 2021) . **Figure 5** illustrates this comparative strength development for M30 (w/b = 0.50) and M50 (w/b = 0.35) concrete grades

The higher specific surface area of calcined clay requires approximately 30–50% higher polycarboxylate-ether (PCE) superplasticiser dosage to achieve equivalent workability at equivalent w/b ratio (Ferreiro et al., 2017; Hay & Celik, 2023) . This additional SP demand has a direct economic cost impact that must be factored into comparative cost assessments (Section 7.4). Curing temperature is the most significant practical constraint on early-age strength development: at 10°C, LC3 pozzolanic kinetics are sufficiently suppressed that OPC strength equivalence may not be achieved by 28 days, with strengths falling to 75–85% of those achieved at 20°C curing under equivalent mix design(Hay & Celik, 2023; Zunino et al., 2022) demonstrated that low-reactivity kaolinitic clays can be enhanced through combined PCE optimisation and extended 14-day wet curing, recovering a significant portion of the early-age deficit.

5.2 Elastic Modulus and Design Code Implications

The elastic modulus of LC3 concrete at 28 days is typically 5–10% lower than OPC at equivalent compressive strength grade, consistent with lower paste stiffness from reduced clinker content and higher gel porosity at early ages. This discrepancy is practically significant for serviceability-controlled designs. (Joseph et al., 2023) confirmed that standard design code expressions for elastic modulus overestimate LC3 elastic modulus by 5–12% at 28 days, while converging to within ±3% at 90 days as pore refinement reduces gel porosity and increases paste stiffness. The practical design implication, corroborated by(Kanavaris et al., 2023) , is that serviceability calculations relying on code elastic modulus expressions should apply a correction factor of 0.90–0.95 for LC3-50 concrete at ages below 56 days, reverting to unity at 90 days and beyond. This convergence occurs because late-age LC3 produces a denser paste through ongoing pozzolanic reaction, while OPC hydration increasingly slows at high degrees of hydration.

5.3 Creep and Shrinkage

(Ston & Scrivener, 2019) conducted the first dedicated study of basic creep in LC3 paste, finding approximately 28–30% lower basic creep compliance than OPC references at equivalent loading duration, attributed to the denser and more cross-linked C-(A)-S-H gel produced by Al-substitution. The practical consequence of lower creep compliance, if confirmed at concrete scale, would include reduced long-term deflections in flexural members and reduced prestress losses in prestressed elements. However, Joseph et al. (2023) explicitly identified that concrete-scale creep data compatible with EC2 Annex B or ACI 209 formulations remain absent for LC3 across all studied mix designs. The practical implication is that early-age restraint cracking risk is elevated for LC3 in exposed, dry environments but comparable for sealed or well-cured structural elements.

Table 3 : Mechanical and durability performance of LC3, OPC, and FA30 mixes

Binder / Mix	w/b	Age (d)	Comp. Str. (MPa)	Cl Diff. (×10⁻¹² m²/s)	Resistivity (kΩ·cm)	E-Mod. (GPa)
OPC (M30)	0.50	28	38	12.0	5.1	32.5
LC3-50 (55% MK)	0.50	28	37	0.42	68	30.8
LC3-50 (55% MK)	0.50	90	43	0.18	145	32.6
LC3-50 (40% MK)	0.45	28	41	0.65	55	30.2
LC3-50 (95% MK)	0.45	28	44	0.11	180	31.5
LC3-30	0.50	28	35	1.85	28	31.0
LC3-50	0.35	28	51	0.30	72	33.2
FA30 (reference)	0.50	28	32	3.20	14	30.5

Table 4 : Quantitative performance synthesis

Performance Metric	OPC Mean	OPC Range	LC3-50 Mean	LC3-50 Range
Comp. strength 28d (MPa)	38	30–52	37	28–55
Comp. strength 90d (MPa)	40	33–55	43	35–62
Elastic modulus 28d (GPa)	32.5	29–38	30.5	27–36
Elastic modulus 90d (GPa)	33.0	30–38	32.5	29–37
Cl diffusivity 28d (×10⁻¹² m²/s)	12.0	8–18	0.35	0.1–1.2
Elec. resistivity 28d (kΩ·cm)	5.5	4–7	72	55–180
Carbonation depth 1yr tropical (mm)	4.2	3–6	7.8	5–12
Basic creep compliance (×10⁻⁶/MPa)	95	80–110	68	55–85
Autogenous shrinkage 90d (με)	118	95–145	165	140–190
Drying shrinkage 365d (με)	420	380–480	370	330–420
GWP cradle-to-gate (kg CO_2-eq/t)	850	820–890	510	480–560

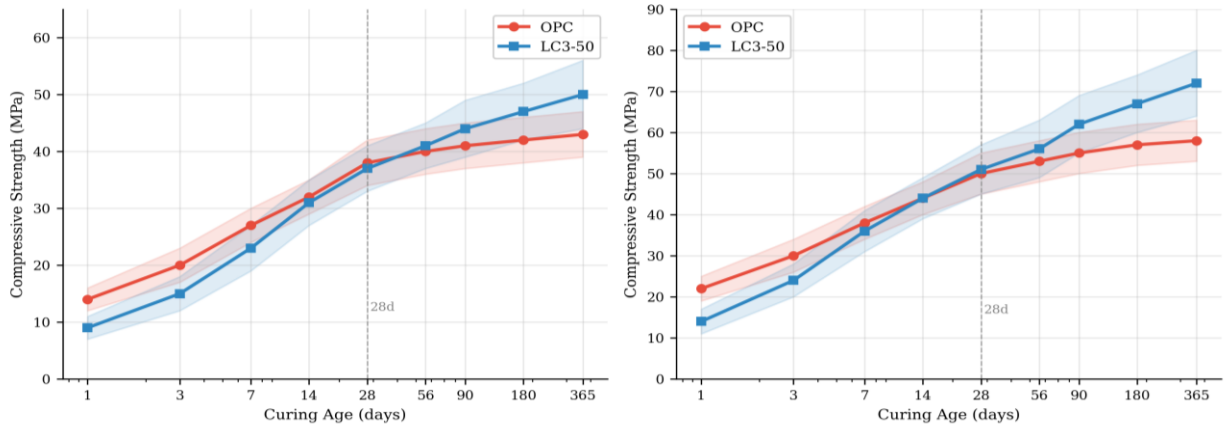

(a) (b)

Figure 5 : Compressive strength development for M30 (w/b = 0.50) and M50 (w/b = 0.35) concrete grades.

6. Durability Performance

Durability performance is the domain in which LC3 provides its most consistently reproducible and transformative advantages over OPC. The dense, discontinuous pore structure established by pozzolanic and

carboaluminate reactions underpins superiority across multiple degradation mechanisms, while the consumption of portlandite creates a managed susceptibility to carbonation that requires specific design attention.

6.1 Chloride Transport and Service Life

Chloride-induced reinforcement corrosion is the dominant durability failure mechanism for concrete structures in marine and de-icing salt environments globally.(Maraghechi et al., 2018) conducted the most comprehensive kaolinite-resolved chloride transport study, testing five calcined clays spanning kaolinite contents of 17–95% in LC3-50 systems at w/b = 0.50. Their central finding was that an intermediate kaolinite content of approximately 50% already achieves approximately two orders of magnitude reduction in the non-steady-state chloride migration coefficient (D_{nssm}) relative to plain OPC, falling from approximately 12×10^{-12} m²/s for OPC to 0.42×10^{-12} m²/s for LC3-50. A saturation behaviour was identified above approximately 50% kaolinite, where further diffusivity reduction plateaus, establishing that the greatest return on raw material investment occurs in the 40–60% kaolinite range.(Dhandapani & Santhanam, 2020) established through systematic microstructural characterisation that C-(A)-S-H composition and higher surface charge is the critical factor governing chloride transport. Chemical chloride binding through Friedel's salt and Kuzel's salt formation provides supplementary retardation beyond the dominant physical barrier effect. NT Build 492 (migration) is preferred over ASTM C1202 (RCPT) for comparative LC3 assessments because RCPT is sensitive to the high electrical resistivity of LC3 matrix beyond the chloride binding regime and tends to overestimate the relative benefit (Dhandapani et al., 2024) .(Pillai et al., 2019) demonstrated using Fick's second law service life modelling that LC3 concrete extends chloride-initiated corrosion service life by up to approximately ten times relative to OPC of comparable 28-day compressive strength, with CO_2 per year of marine service reduced by approximately 90% on a functional-unit basis.

6.2 Carbonation Resistance

LC3 systems are inherently more susceptible to carbonation than OPC because the pozzolanic reaction consumes the majority of portlandite, leaving C-(A)-S-H and carboaluminate phases as the primary CO_2 acceptors, which react more slowly with atmospheric CO_2 than crystalline $Ca(OH)_2$ (Khan et al., 2020). (Rathnarajan et al., 2022) provided the most comprehensive long-term evidence base, monitoring natural carbonation in tropical outdoor exposure of 34 concretes over five years. LC3 concrete at equivalent 28-day compressive strength consistently exhibited carbonation depths approximately 1.5–2.5 times greater than OPC in tropical climate exposure. A critical methodological finding was that the conventional 1% CO_2 accelerated carbonation test significantly overestimates natural carbonation rates for LC3 relative to OPC by approximately 3–4 times, because the high CO_2 concentration drives carbonation through AFm and AFt phases not involved at natural exposure concentrations. This methodological incompatibility means accelerated test results for LC3 cannot be used directly for service life prediction without explicit correction factors derived from paired natural exposure data. The carbonation vulnerability is manageable through targeted design: an increase in concrete cover depth of approximately 5–10 mm above OPC requirements is estimated to compensate for the increased carbonation rate in tropical climates.

6.3 Alkali-Silica Reaction Mitigation

LC3 is highly effective at suppressing alkali-silica reaction (ASR) because pozzolanic and carboaluminate reactions substantially reduce the hydroxyl ion concentration of the pore solution. Nguyen et al. (2020) assessed ASR mitigation using the accelerated mortar bar test (AMBT, ASTM C1567) with borosilicate glass as a model reactive aggregate. At 30% clinker substitution by LC3 binder, 14-day mortar bar expansion was reduced to 0.08%, well below the ASTM C1567 harmful threshold of 0.10%, compared with 0.42% expansion in the OPC reference. They additionally revealed that calcium-rich phases in LC3 delay ASR gel formation kinetics and produce ASR products with elevated Ca/Si ratio and reduced expansive capacity, providing a dual mechanism of ASR suppression: pore solution alkalinity reduction and modified gel composition. However, AMBT provides

only a 14-day screening outcome with borosilicate glass and does not capture the behaviour of slowly reactive aggregates, such as greywacke, argillite, and some granites that are the dominant ASR concern in infrastructure construction.

6.4 Sulfate Resistance

Sulfate resistance of LC3 is nuanced and exposure-class dependent. (Shi et al., 2019) investigated LC3-type mortars exposed to 0.11 M Na_2SO_4 at 5°C and 20°C using XRD, TGA, and expansion measurements. At 20°C, the finer pore structure of LC3 retards sulfate ingress, providing adequate resistance for standard XA1 exposure class. At 5°C, thermodynamic modelling (Lothenbach et al., 2008) confirmed and XRD analysis detected thaumasite (TSA) formation within AFm phases, representing a material safety concern for LC3 specifications in substructure elements in cold climates with sulfate-bearing groundwater. For practical design, the following protocol is recommended: LC3-50 is suitable for XA1 exposure at ambient temperatures above 10°C without restriction; XA2 and XA3 exposure classes in cold climates (≤10°C) carry TSA risk, and LC3 should be specified with caution in these contexts with supplementary XRD monitoring recommended for critical infrastructure.

6.5 Reinforcement Corrosion

(Nguyen & Castel, 2020) conducted the most comprehensive long-term corrosion study, monitoring open circuit potential, linear polarisation resistance, and corrosion current density in both chloride-induced and carbonation-induced scenarios over 500 days. For chloride-induced corrosion propagation, LC3 showed approximately 60–70% lower corrosion current density throughout the propagation phase, consistent with substantially higher resistivity of the LC3 matrix. The electrochemical mechanism underlying this reduction was elucidated by (Stefanoni et al., 2019) , who demonstrated that corrosion rate in dense porous media is governed by the critical pore size for capillary condensation of the electrolyte film at the steel surface: in LC3's nanoporous matrix, this film is thinner, reducing both anodic and cathodic kinetics simultaneously. For carbonation-induced corrosion, propagation rates in LC3 and OPC were comparable once carbonation had depassivated the steel, because subsequent corrosion rate is governed by resistivity and oxygen availability in the carbonated zone rather than by uncarbonated bulk matrix chemistry (Nguyen & Castel, 2020). A critical knowledge gap identified in this review is the complete absence of measured critical chloride threshold (C_n^{RIT}) values specific to LC3 paste and concrete compositions. (Angst et al., 2009) established the fundamental variability of C_n^{RIT} in OPC systems (0.4–2.5% by weight of cement) and its role as the dominant source of service life prediction uncertainty.

6.6 Fire and Elevated Temperature Resistance

(Lin et al., 2021) conducted the first systematic macro-meso-micro investigation of LC3 paste under elevated temperature, establishing the phase decomposition sequence: evaporable water loss and Hc/Mc dehydration at 100–250°C; portlandite decomposition at 400–500°C; calcite decarbonation at 600–800°C; high-temperature phases above 900°C. A key distinction from OPC is that LC3 contains substantially less portlandite due to extensive pozzolanic consumption, which reduces crack initiation severity in the 400–500°C range where portlandite decomposition is most destructive in OPC systems. They also confirmed reduced microcrack density in LC3 paste at 500°C compared with equivalent OPC paste examined by SEM, and residual compressive strength after exposure at 200–600°C was comparable across binder types, suggesting that total porosity and aggregate-paste interface quality govern macro-scale fire performance at these temperatures.

6.7 Freeze-Thaw Resistance

Freeze-thaw resistance represents the most critical and least investigated single knowledge gap in the LC3 durability evidence base. The RILEM TC 282-CCL durability review (Dhandapani et al., 2024) explicitly identified the absence of standardised freeze-thaw data as a critical limitation, and (Shamseldein et al., 2025) confirmed through bibliometric analysis that freeze-thaw durability is the least published LC3 topic in the global

literature. The theoretical concern is mechanistically grounded.(Powers, 1945) established that hydraulic pressure generated by ice formation in saturated capillary pores is the primary frost damage mechanism in concrete and that an adequate spacing factor for entrained air voids ($\bar{d} \leq 0.20$ mm) is the primary engineering safeguard. In LC3, the critical pore entry diameter of 10–30 nm at 28 days generates substantially higher osmotic pressure during freeze-thaw cycling compared with OPC. Water freezes at significantly depressed temperatures in pores below approximately 50 nm diameter (the Kelvin depression effect), meaning that LC3's refined pore system may be less susceptible to bulk hydraulic pressure but more susceptible to micro-ice lens formation associated with osmotic pressure differentials between frozen and unfrozen pore domains. Air entrainment may also be less effective in LC3 because the refined pore structure alters the pressure relief geometry that entrained air voids provide.

7. Environmental and Economic Performance

Environmental and economic performance constitute the primary analytical lens through which LC3 is evaluated in the Journal of Cleaner Production context. This section synthesises evidence from life cycle assessment, functional-unit analysis, water and energy footprints, and production economics, establishing the multi-dimensional sustainability case for LC3 as a cleaner cement technology.

7.1 Life Cycle Assessment and Global Warming Potential

Multiple independent LCA studies converge on 30–40% GWP reduction per tonne of binder for LC3-50 relative to OPC at the cradle-to-gate boundary (Table 5). Sánchez Berriel et al. (2016) conducted the foundational LCA study in Cuba using the ReCiPe midpoint method, quantifying approximately 38% GWP reduction for LC3-50 (510 vs 850 kg CO_2-eq per tonne). A comparative cradle-to-gate GWP summary across binder types is presented in **Figure 6**. The primary drivers are the elimination of limestone decarbonation from the displaced clinker fraction and substantially lower thermal energy demand of clay calcination (~900°C) relative to clinker production (~1450°C). Thermal energy demand is consequently reduced by approximately 25–28% in fossil-fuel-based contexts: clay calcination produces approximately 0.08–0.12 kg CO_2 per kg of calcined clay (fuel combustion only; no process decarbonation) compared with approximately 0.53–0.57 kg CO_2 per kg of clinker including both process and combustion emissions (Sánchez Berriel et al., 2016). In a renewable energy scenario where clay calcination is powered by electrified kilns with zero-carbon electricity, the GWP of LC3-50 could approach 125 kg CO_2-eq per tonne (Habert et al., 2020). Waste-derived calcined clays using system expansion LCA approach zero or negative effective GWP through avoided-burden credits (Amar et al., 2024). Cancio Díaz et al. (2017) demonstrated that new OPC plant construction carries prohibitive environmental impact across all LCA categories compared with LC3 kiln retrofit.

7.2 Functional-Unit LCA: GWP per Year of Structural Service

The most powerful environmental argument for LC3 emerges when life cycle assessment is expressed on a functional unit basis rather than per tonne of binder.(Pillai et al., 2019) quantified CO_2 emissions per unit of concrete per year of estimated service life for bridge pier and girder elements in marine environments, demonstrating that the combined effect of lower production GWP and dramatically extended service life reduces CO_2 per year of marine structural service to approximately 85 kg CO_2-eq for LC3-50 versus approximately 850 kg CO_2-eq for OPC of comparable strength. This approximately 90% reduction per functional unit arises from the multiplicative interaction of the 30–40% production GWP reduction and the up to 10-fold service life extension demonstrated by (Pillai et al., 2019). (Habert et al., 2020) contextualised this at global scale: if LC3 were to displace 20% of global OPC production, the annual CO_2-eq savings would be approximately 265 million tonnes, equivalent to grounding the entire global commercial aviation fleet for one year. This functional-unit framing fundamentally changes the economic and policy logic of LC3 adoption and should constitute the primary metric for infrastructure procurement decisions in marine and chloride-exposed environments.

7.3 Water Footprint and Broader Environmental Impact Categories

Beyond GWP, LCA of LC3 reveals advantages across multiple additional environmental impact categories that have received insufficient attention in prior reviews. Water consumption in LC3 production is approximately 15–20% lower than OPC per tonne of cement, because clay calcination requires less process water than wet-process clinker circuits and kiln cooling systems (Habert et al., 2020). Acidification potential, driven primarily by SO_2 and NO_x emissions from kiln combustion, is reduced proportionally to the reduction in fuel consumption. Embodied energy (primary energy demand) is reduced by 20–25% per tonne of binder (Habert et al., 2020). These co-benefits reinforce the multi-dimensional sustainability advantage of LC3 beyond the primary climate metric. For waste-derived calcined clay pathways such as the Grand Paris Express soils case (Amar et al., 2024) , the circular economy avoided-burden credits across these additional categories compound the environmental advantage to a degree that may make waste-derived LC3 the most comprehensively sustainable binder option across all categories simultaneously.

7.4 Economic Performance and Deployment Economics

In clinker-dominated cost structures typical of emerging economies, replacing 50% of clinker with calcined clay and limestone reduces cement production cost by approximately 10–15% per tonne, because calcined clay and limestone are both significantly less expensive than clinker per unit mass (Krishnan et al., 2019) ((Sánchez Berriel et al., 2016) . The capital investment for calciner installation at an existing cement plant is estimated at USD 5–15 million per 100,000 tonnes per year of LC3 production capacity, substantially lower than the USD 80–200 million required for a new clinker line of equivalent capacity (Cancio Díaz et al., 2017). Return on capital employed (ROCE) for LC3 retrofit projects in India and Cuba has been estimated at 15–25% per annum in independent analyses, driven by the combination of lower raw material cost and premium market positioning relative to standard OPC(Krishnan et al., 2019);(Cancio Díaz et al., 2017). The primary economic barriers to LC3 adoption are institutional and market-access constraints rather than production cost disadvantages: the absence of LC3-specific clauses in ASTM C595 creates liability concerns; conservative clinker content minima in EN 197-5 preclude direct specification in European markets without performance-based approval; and absence of LC3-specific durability design tables in major structural codes forces project-specific testing that adds cost and delays (Kanavaris et al., 2023) . Cost sensitivity analysis shows that at PCE superplasticiser prices above approximately USD 1,800 per tonne, the additional SP demand of LC3 mixes narrows the cost advantage to 5–8%, still economically favourable but less compelling in high-plasticiser-cost markets (Hay & Celik, 2023) .

Table 5 : Life cycle assessment and global warming potential comparison across primary LC3 studies

Binder System	GWP (kg CO_2/t)	Reduction vs OPC	Thermal Energy (GJ/t)	Elec. Energy (kWh/t)	LCA Method
OPC (reference)	850	—	3.2	~35	ReCiPe
LC3-30	595	–30%	2.5	30	ReCiPe
LC3-50	510	–40%	2.3	32	CML 2002
LC3-50 (renewable)	125	–85%	~0	~0	Scenario
LC3-50 (waste clay)	≤0	>–91%	2.0	28	System exp.
FA30 (reference)	595	–30%	2.9	33	CML 2002
GGBS30 (reference)	595	–30%	2.8	34	CML 2002
LC3-50 (per yr marine)	~85	–~90%	—	—	Functional unit

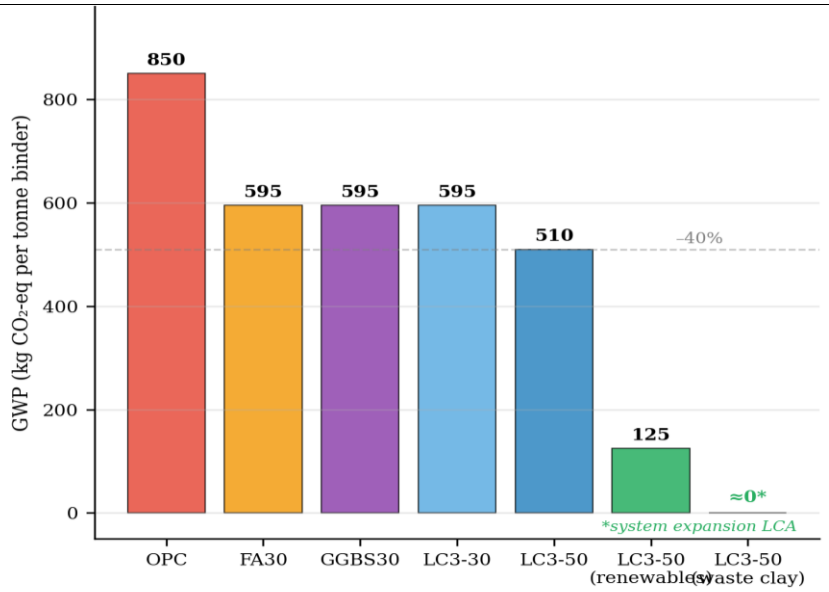

Figure 6 : Cradle-to-gate GWP comparison across binder types

8. Industrial Deployment and Field Performance

LC3 has progressed from laboratory concept in 2012 to commercial production across multiple continents, representing one of the most rapid laboratory-to-industry transitions in cement technology (Parashar et al., 2024)

Cuba's Siguaney Cement Factory achieved the first industrial-scale production in 2013 with modest modifications to an existing wet-process kiln (Almenares et al., 2017) . Compressive strengths exceeded 35 MPa at 28 days with full compatibility with existing construction practice (Vizcaíno Andrés et al., 2015). Cuba's NC 506 standard was amended to accommodate LC3, establishing the first national regulatory framework(Kanavaris et al., 2023).

India's LC3 development, led by IIT Delhi and IIT Madras, scaled to three industrial locations, confirming that Blaine fineness, R3 reactivity, and 7-day mortar strength are adequate for batch qualification with no construction changes above 15°C (Krishnan et al., 2019) . Full commercial production at JK Lakshmi Cement's Rajasthan plant, supplying the Noida International Airport project with approximately 50,000 tonnes of LC3 binder (Parashar et al., 2024) . This experience demonstrated that standardisation preceding or simultaneous with commercial scale-up is the most effective regulatory pathway.

Colombia's Argos Rioclaro plant became the first independent large-scale calcined clay facility outside the EPFL-IIT-Cuba network, confirming commercial reproducibility without direct technology transfer. In Sub-Saharan Africa, feasibility was confirmed for Kenyan raw materials (Marangu, 2020) and fully demonstrated in Malawi using locally sourced materials, with 28-day strengths meeting local structural grade requirements (Kafodya et al., 2023) . Sub-Saharan Africa and Southeast Asia offer the greatest per-unit CO_2 reduction per investment due to heavy reliance on new cement production and limited fly ash/GGBS access.

9. Current Challenges and Research Roadmap

LC3 faces six priority gaps (freeze-thaw, creep, Ccrit, fire, non-tropical carbonation, and cold-weather curing) organised into three implementation horizons.

Technical: Freeze-thaw resistance is the highest-severity gap; elevated osmotic pressure from the refined pore structure combined with zero standardised test data prevents specification in frost climates. Concrete-scale creep coefficients for EC2/ACI 209 are absent despite 30% lower paste-level compliance.

Standardisation: Carbonation cover depth tables exist only for tropical climates; temperate/cold data are absent. Cold-weather curing below 15°C has only one published study. Prescriptive barriers in ASTM C595/EN 197-5 persist, though performance-based revision enabled by IS 18189:2023 offers a path forward.

Practical barriers: Reddish-brown colouration, SP demand variability requiring unstandardised PCE dosing, limited training in emerging markets, and supply chain gaps for calcination equipment. Lower heat of hydration complicates OPC-derived thermal management protocols for mass concrete.

Immediate priorities: Establish freeze-thaw testing (three air contents: 1.5%, 3.5%, 6.0%; two aggregates; three grades: C25/30–C45/55; CEN/TS 12390-9 and ASTM C666). Develop cold-weather protocols (5–20°C in 5°C increments; Type-C accelerators; 60°C steam curing). Conduct 18-month creep tests (M25–M50; 30% and 60% f'c) to calibrate EC2/ACI 209. Determine Ccrit via polarisation across four w/b ratios and three kaolinite contents. Establish an open-data platform for AI/ML development.

Medium-term priorities: Characterise fire performance (200–900°C; 100°C increments) for EN 1992-1-2 kc(θ)/kE(θ). Generate carbonation tables for temperate/cold climates via ≥ six-zone international exposure. Characterise quaternary LC3 blends with residual GGBS, fly ash, or silica fume. Quantify adiabatic temperature rise for mass concrete thermal modelling. Revise ASTM C595/EN 197-5 using Horizon 1–2 data.

Strategic priorities: Develop AI/ML mix design models linking clay mineralogy to performance. Aggregate a 10-year field database from ≥50 global deployment sites. Advance electrified calcination (renewable-powered) to reduce LC3-50 GWP below 150 kg CO_2-eq/t. Build a durability-based design framework (ISO 13823/fib Bulletin 34) integrating diffusivity, carbonation, and Ccrit. Full deployment at 20–30% of global cement output would cut annual CO_2 by 800–900 Mt.

10.Conclusions

This PRISMA 2020-compliant systematic review synthesised 66 peer-reviewed studies on calcined clay as a supplementary cementitious material. The following conclusions are supported by the evidence:

1. Kaolinite content is the primary determinant of pozzolanic activity. The ASTM C618 75% PAI threshold is reliably met above approximately 40% kaolinite with optimised calcination at 650–850°C. Clays with 40–50% kaolinite deliver full LC3 performance at substantially lower cost than high-grade kaolinite.
2. Soak and flash calcination yield equivalent pozzolanic reactivity at equal dehydroxylation degree and particle size; route choice is secondary to kaolinite content. Overcalcination above approximately 950°C reduces reactivity through Al–Si spinel formation, detectable by DSC. Waste-derived calcined clays offer near-zero or negative GWP under system expansion LCA.
3. The synergistic metakaolin–limestone reaction forms hemicarbonate and monocarbonate, stabilises ettringite, increases total hydrate volume, and refines critical pore entry diameter from 80–120 nm (OPC) to 10–30 nm (LC3-50) at 28 days. Portlandite is largely consumed by 28–56 days; late-age strength gain is capillary-transport-limited.
4. LC3-50 reaches OPC-equivalent 28-day compressive strength and exceeds OPC beyond 28 days. Elastic modulus is 5–10% below OPC at 28 days but converges by 90 days; a correction factor of 0.90–0.95 is recommended for EC2/ACI serviceability below 56 days. Basic creep compliance is approximately 28–30% lower than OPC at paste level. Cold-weather curing below 15°C is the principal early-age limitation.
5. LC3-50 demonstrates superiority over OPC in five performance dimensions: chloride resistance, ASR mitigation, creep, GWP, and production cost (10–15% lower).
6. LC3-50 reduces cradle-to-gate GWP by 30–40% per tonne of binder, with 85% reduction achievable under renewable calcination and near-zero/negative GWP for waste-derived clays.
7.

References

Alameri, I., & Oltulu, M. (2020a). Bond Strength Between Concrete Substrate and Reinforced Polyester Composites. *Journal of Materials Engineering and Performance*, *30*(1), 56–65. https://doi.org/10.1007/s11665-020-05295-7

Alameri, I., & Oltulu, M. (2020b). Mechanical properties of polymer composites reinforced by silica-based materials of various sizes. *Applied Nanoscience*, *10*(11), 4087–4102. https://doi.org/10.1007/s13204-020-01516-6

Alameri, I., & Oltulu, M. (2023). Experimental and numerical study on the mechanical properties of reinforced polyester composites. *Advances in Materials Research*, *12*(3), 227–242. https://doi.org/10.12989/amr.2023.12.3.227

Almenares, R. S., Vizcaíno, L. M., Damas, S., Mathieu, A., Alujas, A., & Martirena, F. (2017). Industrial calcination of kaolinitic clays to make reactive pozzolans. *Case Studies in Construction Materials*, *6*, 225–232. https://doi.org/10.1016/j.cscm.2017.03.005

Alujas, A., Fernández, R., Quintana, R., Scrivener, K. L., & Martirena, F. (2015). Pozzolanic reactivity of low grade kaolinitic clays: Influence of calcination temperature and impact of calcination products on OPC hydration. *Applied Clay Science*, *108*, 94–101. https://doi.org/10.1016/j.clay.2015.01.028

Alujas Diaz, A., Almenares Reyes, R. S., Hanein, T., Irassar, E. F., Juenger, M., Kanavaris, F., Maier, M., Marsh, A. T., Sui, T., Thienel, K.-C., Valentini, L., Wang, B., Zunino, F., & Snellings, R. (2022). Properties and occurrence of clay resources for use as supplementary cementitious materials: a paper of RILEM TC 282-CCL. *Materials and Structures*, *55*(5), 139. https://doi.org/10.1617/s11527-022-01972-2

Amar, M., Kleib, J., Tall, M., Alloul, A., Zeraoui, A., Abriak, N.-e., & Benzerzour, M. (2024). Case study: reuse of excavated soils from the Grand Paris Express project for the formulation of low-carbon cementitious matrixes. *Journal of Material Cycles and Waste Management*, *26*(4), 2579–2590. https://doi.org/10.1007/s10163-024-01957-z

Angst, U., Elsener, B., Larsen, C. K., & Vennesland, Ø. (2009). Critical chloride content in reinforced concrete — A review. *Cement and Concrete Research*, *39*(12), 1122–1138. https://doi.org/10.1016/j.cemconres.2009.08.006

Antoni, M., Rossen, J., Martirena, F., & Scrivener, K. (2012). Cement substitution by a combination of metakaolin and limestone. *Cement and Concrete Research*, *42*(12), 1579–1589. https://doi.org/10.1016/j.cemconres.2012.09.006

Avet, F., & Scrivener, K. (2018). Investigation of the calcined kaolinite content on the hydration of Limestone Calcined Clay Cement (LC3). *Cement and Concrete Research*, *107*, 124–135. https://doi.org/10.1016/j.cemconres.2018.02.016

Avet, F., Snellings, R., Alujas Diaz, A., Ben Haha, M., & Scrivener, K. (2016). Development of a new rapid, relevant and reliable (R3) test method to evaluate the pozzolanic reactivity of calcined kaolinitic clays. *Cement and Concrete Research*, *85*, 1–11. https://doi.org/10.1016/j.cemconres.2016.02.015

Baki, V. A., Ke, X., Heath, A., Calabria-Holley, J., Terzi, C., & Sirin, M. (2022). The impact of mechanochemical activation on the physicochemical properties and pozzolanic reactivity of kaolinite, muscovite and montmorillonite. *Cement and Concrete Research*, *162*, 106962. https://doi.org/10.1016/j.cemconres.2022.106962

Briki, Y., Avet, F., Zajac, M., Bowen, P., Haha, M. B., & Scrivener, K. (2021). Understanding of the factors slowing down metakaolin reaction in limestone calcined clay cement (LC3) at late ages. *Cement and Concrete Research*, *146*, 106477. https://doi.org/10.1016/j.cemconres.2021.106477

Cancio Díaz, Y., Sánchez Berriel, S., Heierli, U., Favier, A. R., Sánchez Machado, I. R., Scrivener, K. L., Martirena Hernández, J. F., & Habert, G. (2017). Limestone calcined clay cement as a low-carbon solution to meet expanding cement demand in emerging economies. *Development Engineering*, *2*, 82–91. https://doi.org/10.1016/j.deveng.2017.06.001

De Weerdt, K., Haha, M. B., Le Saout, G., Kjellsen, K. O., Justnes, H., & Lothenbach, B. (2011). Hydration mechanisms of ternary Portland cements containing limestone powder and fly ash. *Cement and Concrete Research*, *41*(3), 279–291. https://doi.org/10.1016/j.cemconres.2010.11.014

Dhandapani, Y., Machner, A., Wilson, W., Kunther, W., Afroz, S., Kim, T., Zunino, F., Joseph, S., Kanavaris, F., Castel, A., Thienel, K. C., Irassar, E. F., Bishnoi, S., Martirena, F., & Santhanam, M. (2024). Performance of cementitious systems containing calcined clay in a chloride-rich environment: a review by TC-282 CCL. *Mater Struct*, *57*(7), 154. https://doi.org/10.1617/s11527-024-02426-7

Dhandapani, Y., Sakthivel, T., Santhanam, M., Gettu, R., & Pillai, R. G. (2018). Mechanical properties and durability performance of concretes with Limestone Calcined Clay Cement (LC3). *Cement and Concrete Research*, *107*, 136–151. https://doi.org/10.1016/j.cemconres.2018.02.005

Dhandapani, Y., & Santhanam, M. (2020). Investigation on the microstructure-related characteristics to elucidate performance of composite cement with limestone-calcined clay combination. *Cement and Concrete Research*, *129*, 105959. https://doi.org/10.1016/j.cemconres.2019.105959

Dixit, A., Du, H., & Pang, S. D. (2021). Performance of mortar incorporating calcined marine clays with varying kaolinite content. *Journal of Cleaner Production*, *282*, 124513. https://doi.org/10.1016/j.jclepro.2020.124513

Fernandez, R., Martirena, F., & Scrivener, K. L. (2011). The origin of the pozzolanic activity of calcined clay minerals: A comparison between kaolinite, illite and montmorillonite. *Cement and Concrete Research*, *41*(1), 113–122. https://doi.org/10.1016/j.cemconres.2010.09.013

Ferreiro, S., Herfort, D., & Damtoft, J. S. (2017). Effect of raw clay type, fineness, water-to-cement ratio and fly ash addition on workability and strength performance of calcined clay – Limestone Portland cements. *Cement and Concrete Research*, *101*, 1–12. https://doi.org/10.1016/j.cemconres.2017.08.003

Habert, G., Miller, S. A., John, V. M., Provis, J. L., Favier, A., Horvath, A., & Scrivener, K. L. (2020). Environmental impacts and decarbonization strategies in the cement and concrete industries. *Nature Reviews Earth & Environment*, *1*(11), 559–573. https://doi.org/10.1038/s43017-020-0093-3

Hanein, T., Thienel, K.-C., Zunino, F., Marsh, A. T. M., Maier, M., Wang, B., Canut, M., Juenger, M. C. G., Ben Haha, M., Avet, F., Parashar, A., Al-Jaberi, L. A., Almenares-Reyes, R. S., Alujas-Diaz, A., Scrivener, K. L., Bernal, S. A., Provis, J. L., Sui, T., Bishnoi, S., & Martirena-Hernández, F. (2021). Clay calcination technology: state-of-the-art review by the RILEM TC 282-CCL. *Materials and Structures*, *55*(1), 3. https://doi.org/10.1617/s11527-021-01807-6

Hay, R., & Celik, K. (2023). Effects of water-to-binder ratios (w/b) and superplasticizer on physicochemical, microstructural, and mechanical evolution of limestone calcined clay cement (LC3). *Construction and Building Materials*, *391*, 131529. https://doi.org/10.1016/j.conbuildmat.2023.131529

Hollanders, S., Adriaens, R., Skibsted, J., Cizer, Ö., & Elsen, J. (2016). Pozzolanic reactivity of pure calcined clays. *Applied Clay Science*, *132-133*, 552–560. https://doi.org/10.1016/j.clay.2016.08.003

Joseph, S., Dhandapani, Y., Geddes, D. A., Zhao, Z., Bishnoi, S., Vieira, M., Martirena, F., Castel, A., Kanavaris, F., Bansal, T., & Riding, K. A. (2023). Mechanical properties of concrete made with calcined clay: a review by RILEM TC-282 CCL. *Materials and Structures*, *56*(4), 84. https://doi.org/10.1617/s11527-023-02118-8

Juenger, M. C. G., Snellings, R., & Bernal, S. A. (2019). Supplementary cementitious materials: New sources, characterization, and performance insights. *Cement and Concrete Research*, *122*, 257–273. https://doi.org/10.1016/j.cemconres.2019.05.008

Kafodya, I., Basuroy, D., Marangu, J. M., Kululanga, G., Maddalena, R., & Novelli, V. I. (2023). Mechanical Performance and Physico-Chemical Properties of Limestone Calcined Clay Cement (LC3) in Malawi. *Buildings*, *13*(3), 740. https://doi.org/10.3390/buildings13030740

Kanavaris, F., Vieira, M., Bishnoi, S., Zhao, Z., Wilson, W., Tagnit Hamou, A., Avet, F., Castel, A., Zunino, F., Visalakshi, T., Martirena, F., Bernal, S. A., Juenger, M. C. G., & Riding, K. (2023). Standardisation of low clinker cements containing calcined clay and limestone: a review by RILEM TC-282 CCL. *Materials and Structures*, *56*(9), 169. https://doi.org/10.1617/s11527-023-02257-y

Khan, M. S. H., Nguyen, Q. D., & Castel, A. (2020). Performance of limestone calcined clay blended cement-based concrete against carbonation. *Advances in Cement Research*, *32*(11), 481–491. https://doi.org/10.1680/jadcr.18.00172

Koutsouradi, A., Leal da Silva, W. R., Damø, A. J., & Jensen, P. A. (2025). Experimental investigation and comparison of soak and flash calcined kaolinite and montmorillonite. *Applied Clay Science*, *265*, 107649. https://doi.org/10.1016/j.clay.2024.107649

Krishnan, S., Emmanuel, A. C., Shah, V., Parashar, A., Mishra, G., Maity, S., & Bishnoi, S. (2019). Industrial production of limestone calcined clay cement: experience and insights. *Green Materials*, *7*(1), 15–27. https://doi.org/10.1680/jgrma.18.00003

Lin, R.-S., Han, Y., & Wang, X.-Y. (2021). Macro–meso–micro experimental studies of calcined clay limestone cement (LC3) paste subjected to elevated temperature. *Cement and Concrete Composites*, *116*, 103871. https://doi.org/10.1016/j.cemconcomp.2020.103871

Lothenbach, B., Matschei, T., Möschner, G., & Glasser, F. P. (2008). Thermodynamic modelling of the effect of temperature on the hydration and porosity of Portland cement. *Cement and Concrete Research*, *38*(1), 1–18. https://doi.org/10.1016/j.cemconres.2007.08.017

Lothenbach, B., Scrivener, K., & Hooton, R. D. (2011). Supplementary cementitious materials. *Cement and Concrete Research*, *41*(12), 1244–1256. https://doi.org/10.1016/j.cemconres.2010.12.001

Manosa, J., Calderon, A., Salgado-Pizarro, R., Maldonado-Alameda, A., & Chimenos, J. M. (2024). Research evolution of limestone calcined clay cement (LC(3)), a promising low-carbon binder - A comprehensive overview. *Heliyon*, *10*(3), e25117. https://doi.org/10.1016/j.heliyon.2024.e25117

Maraghechi, H., Avet, F., Wong, H., Kamyab, H., & Scrivener, K. (2018). Performance of Limestone Calcined Clay Cement (LC3) with various kaolinite contents with respect to chloride transport. *Materials and Structures*, *51*(5), 125. https://doi.org/10.1617/s11527-018-1255-3

Marangu, J. M. (2020). Physico-chemical properties of Kenyan made calcined Clay -Limestone cement (LC3). *Case Studies in Construction Materials*, *12*, e00333. https://doi.org/10.1016/j.cscm.2020.e00333

Martirena Hernández, J. F., Antoni, M., Oquendo-Machado, Y., Borrajo-Perez, R., Alujas-Diaz, A., & Almenares-Reyes, R. (2024). Impact of calcination technology on properties of calcined clays. *RILEM Technical Letters*, *8*, 190–197. https://doi.org/10.21809/rilemtechlett.2023.194

Nguyen, Q. D., & Castel, A. (2020). Reinforcement corrosion in limestone flash calcined clay cement-based concrete. *Cement and Concrete Research*, *132*, 106051. https://doi.org/10.1016/j.cemconres.2020.106051

Nguyen, Q. D., Kim, T., & Castel, A. (2020). Mitigation of alkali-silica reaction by limestone calcined clay cement (LC3). *Cement and Concrete Research*, *137*, 106176. https://doi.org/10.1016/j.cemconres.2020.106176

Overmann, S., Vollpracht, A., & Matschei, T. (2024). Reactivity of Calcined Clays as SCM-A Review. *Materials (Basel)*, *17*(2), 312. https://doi.org/10.3390/ma17020312

Page, M. J., McKenzie, J. E., Bossuyt, P. M., Boutron, I., Hoffmann, T. C., Mulrow, C. D., Shamseer, L., Tetzlaff, J. M., Akl, E. A., Brennan, S. E., Chou, R., Glanville, J., Grimshaw, J. M., Hrobjartsson, A., Lalu, M. M., Li, T., Loder, E. W., Mayo-Wilson, E., McDonald, S.,…Moher, D. (2021). The PRISMA 2020 statement: an updated guideline for reporting systematic reviews. *BMJ*, *372*, n71. https://doi.org/10.1136/bmj.n71

Parashar, A., Avet, F., Canut, M., Riding, K. A., Wang, B., Sui, T., Vieira, S., Irassar, E. F., Velasquez, L., Almenares-Reyes, R. S., Thienel, K.-C., Maier, M., Kanavaris, F., Zunino, F., Escadeillas, G., Haha, M. B., Juenger, M. C. G., Hanein, T., Bishnoi, S., & Martirena-Hernández, F. (2024). Industrialisation of calcined clay cements: past, present, and future: a paper of RILEM TC 282-CCL. *Materials and Structures*, *57*(9), 211. https://doi.org/10.1617/s11527-024-02488-7

Pillai, R. G., Gettu, R., Santhanam, M., Rengaraju, S., Dhandapani, Y., Rathnarajan, S., & Basavaraj, A. S. (2019). Service life and life cycle assessment of reinforced concrete systems with limestone calcined clay cement (LC3). *Cement and Concrete Research*, *118*, 111–119. https://doi.org/10.1016/j.cemconres.2018.11.019

Powers, T. C. (1945). A Working Hypothesis for Further Studies of Frost Resistance of Concrete. *ACI Journal Proceedings*, *41*(1), 245–272. https://doi.org/10.14359/8684

Rathnarajan, S., Dhanya, B. S., Pillai, R. G., Gettu, R., & Santhanam, M. (2022). Carbonation model for concretes with fly ash, slag, and limestone calcined clay - using accelerated and five - year natural exposure data. *Cement and Concrete Composites*, *126*, 104329. https://doi.org/10.1016/j.cemconcomp.2021.104329

Sánchez Berriel, S., Favier, A., Rosa Domínguez, E., Sánchez Machado, I. R., Heierli, U., Scrivener, K., Martirena Hernández, F., & Habert, G. (2016). Assessing the environmental and economic potential of Limestone Calcined Clay Cement in Cuba. *Journal of Cleaner Production*, *124*, 361–369. https://doi.org/10.1016/j.jclepro.2016.02.125

Schneider, M., Romer, M., Tschudin, M., & Bolio, H. (2011). Sustainable cement production—present and future. *Cement and Concrete Research*, *41*(7), 642–650. https://doi.org/10.1016/j.cemconres.2011.03.019

Scrivener, K., Avet, F., Maraghechi, H., Zunino, F., Ston, J., Hanpongpun, W., & Favier, A. (2019). Impacting factors and properties of limestone calcined clay cements (LC3). *Green Materials*, *7*(1), 3–14. https://doi.org/10.1680/jgrma.18.00029

Scrivener, K. L., John, V. M., & Gartner, E. M. (2018). Eco-efficient cements: Potential economically viable solutions for a low-CO2 cement-based materials industry. *Cement and Concrete Research*, *114*, 2–26. https://doi.org/10.1016/j.cemconres.2018.03.015

Shamseldein, A., Shamass, R., & Zhou, X. (2025). Bibliometric Review and Research Evolution on the Durability of LC3 Cement. *ScientificWorldJournal*, *2025*(1), 4832631. https://doi.org/10.1155/tswj/4832631

Sharma, M., Bishnoi, S., Martirena, F., & Scrivener, K. (2021). Limestone calcined clay cement and concrete: A state-of-the-art review. *Cement and Concrete Research*, *149*, 106564. https://doi.org/10.1016/j.cemconres.2021.106564

Shi, Z., Ferreiro, S., Lothenbach, B., Geiker, M. R., Kunther, W., Kaufmann, J., Herfort, D., & Skibsted, J. (2019). Sulfate resistance of calcined clay – Limestone – Portland cements. *Cement and Concrete Research*, *116*, 238–251. https://doi.org/10.1016/j.cemconres.2018.11.003

Snellings, R., Almenares Reyes, R., Hanein, T., Irassar, E. F., Kanavaris, F., Maier, M., Marsh, A. T., Valentini, L., Zunino, F., & Alujas Diaz, A. (2022). Paper of RILEM TC 282-CCL: mineralogical characterization methods for clay resources intended for use as supplementary cementitious material. *Materials and Structures*, *55*(5), 149. https://doi.org/10.1617/s11527-022-01973-1

Snellings, R., Suraneni, P., & Skibsted, J. (2023). Future and emerging supplementary cementitious materials. *Cement and Concrete Research*, *171*, 107199. https://doi.org/10.1016/j.cemconres.2023.107199

Stefanoni, M., Angst, U. M., & Elsener, B. (2019). Kinetics of electrochemical dissolution of metals in porous media. *Nat Mater*, *18*(9), 942–947. https://doi.org/10.1038/s41563-019-0439-8

Ston, J., & Scrivener, K. (2019). Basic creep of limestone–calcined clay cements: An experimental and numerical approach. *Theoretical and Applied Fracture Mechanics*, *103*, 102270. https://doi.org/10.1016/j.tafmec.2019.102270

Sui, H., Wang, B., Chen, Z., Liu, Y., Sagoe-Crentsil, K., & Duan, W. (2024). Optimizing calcination for low-grade calcined kaolinite clay: Reactivity and energy consumption. *Case Studies in Construction Materials*, *21*, e04056. https://doi.org/10.1016/j.cscm.2024.e04056

Tironi, A., Trezza, M. A., Scian, A. N., & Irassar, E. F. (2012). Kaolinitic calcined clays: Factors affecting its performance as pozzolans. *Construction and Building Materials*, *28*(1), 276–281. https://doi.org/10.1016/j.conbuildmat.2011.08.064

Vizcaíno Andrés, L. M., Antoni, M. G., Alujas Diaz, A., Martirena Hernández, J. F., & Scrivener, K. L. (2015). Effect of fineness in clinker-calcined clays-limestone cements. *Advances in Cement Research*, *27*(9), 546–556. https://doi.org/10.1680/jadcr.14.00095

Zheng, D., Liang, X., Cui, H., Tang, W., Liu, W., & Zhou, D. (2022). Study of performances and microstructures of mortar with calcined low-grade clay. *Construction and Building Materials*, *327*, 126963. https://doi.org/10.1016/j.conbuildmat.2022.126963

Zunino, F., Dhandapani, Y., Ben Haha, M., Skibsted, J., Joseph, S., Krishnan, S., Parashar, A., Juenger, M. C. G., Hanein, T., Bernal, S. A., Scrivener, K. L., & Avet, F. (2022). Hydration and mixture design of calcined clay blended cements: review by the RILEM TC 282-CCL. *Materials and Structures*, *55*(9), 234. https://doi.org/10.1617/s11527-022-02060-1

Zunino, F., & Scrivener, K. (2024). Reactivity of kaolinitic clays calcined in the 650 °C–1050 °C temperature range: Towards a robust assessment of overcalcination. *Cement and Concrete Composites*, *146*, 105380. https://doi.org/10.1016/j.cemconcomp.2023.105380

Index of Tables

Index of Figures